Evaluation of Three Different Dental Implants in Ligature-Induced Peri-implantitis in the Beagle Dog. Part II. Histology and Microbiology

Heinrich W. S. Tillmanns, DMD, Dr Med Dent, MS*/
Joachim S. Hermann, DMD, Dr Med Dent**/John C. Tiffee, DDS***/
Ann V. Burgess, BSE****/Roland M. Meffert, DDS*****

The purpose of this study was to evaluate experimental peri-implant breakdown microbiologically, radiographically and histologically. Hydroxyapatite-coated, titanium plasma-sprayed, and titanium alloy surfaces were investigated. Eighty-four implants were placed in 14 beagle dogs. Standardized radiographs and microbiologic samples (DNA) were obtained. Dogs were sacrificed at 3 and 6 months. Undecalcified histologic sections were prepared. Thickness of hydroxyapatite coating, changes in crestal bone height, and marginal changes in osseointegration were measured. Vertical bone loss was computed. Radiographs were analyzed using computer-assisted densitometric image analysis (CADIA). Microbial analysis (DNA) did not clearly favor any of the examined surfaces. CADIA did not show differences among implant surfaces. No significant differences among the three implants were noted for histometry, except the experimental titanium plasma-sprayed surface showed an increase in vertical bone loss 6 months ($P < .05$). Thickness of hydroxyapatite was decreased in active peri-implantitis sites ($P < .05$). Clinical attachment level was shown to be the most sensitive clinical parameter for detecting histologic changes. All implants were equally susceptible to peri-implantitis.
(INT J ORAL MAXILLOFAC IMPLANTS 1998;13:59–68)

Key words: beagle dog, endosseous, hydroxyapatite, implant, machined titanium alloy, peri-implantitis, surface, titanium plasma-sprayed

The potential causes of implant failure are many, but most researchers agree that one specific factor leading to clinical failure of all implant types is peri-implant infection. The accumulation of subgingival plaque, namely a gram-negative, anaerobic flora, is considered to be the main etiologic factor in advanced periodontal[1–5] as well as peri-implant[6–12] disease. Recently, attention has been paid to a limited number of bacterial species, such as *Actinobacillus actinomycetemcomitans* (Aa), *Porphyromonas gingivalis* (Pg), and *Prevotella intermedia* (Pi),[3–5,13] which have been reported to be found at increased levels at diseased implant sites.[6]

A hemidesmosomal epithelial attachment similar to that for teeth has been described adjacent to machined implant surfaces.[14,15] Differences, however, were noted in the area of the connective tissue, where a scarlike connective tissue contact with fibers oriented parallel to the long axis of the implant has been described.[16–18] Therefore, when probing at diseased sites or when using excessive force at healthy sites, the probe tip penetrates virtually to the level of crestal bone.[19,20] For hydroxyapatite- (HA) coated implants, resorption of coatings by inflammatory phagocytosis has been observed.[21,22] Bone loss is apparent, similar to an advanced lesion involving teeth. Computer-assisted densitometric image analysis (CADIA) has been proven to be the most sensitive method to detect even small changes in bone density over time.[23,24]

*Private Practice, Prince George, BC, Canada.
**Visiting Assistant Professor, Department of Periodontics, University of Texas Health Science Center, San Antonio, Texas.
***Postdoctoral Fellow, Department of Pathology, University of Texas Health Science Center, San Antonio, Texas.
****Research Associate, Calcitek, Carlsbad, California.
*****Clinical Professor, Department of Periodontics, University of Texas Health Science Center, San Antonio, Texas.

Reprint requests: *Dr Roland M. Meffert, University of Texas Health Science Center at San Antonio, Dental School, Department of Periodontics, 7703 Floyd Curl Drive, San Antonio, Texas 78284-7894. Fax: (210) 567-6858.*

In the past, the dog model has been used to investigate experimental periodontal[25–27] and peri-implant[18,19,28,29] disease. However, no direct comparison has been carried out among different implant types in the same host. Since the severity of peri-implant breakdown depends on the quality and quantity of the bacterial attack, as well as the individual capacity of the host to respond to the bacterial challenge, it seems important to compare different implants in the same animal.

The purpose of the present study was to monitor and compare microbiologically, radiographically, and histologically the progression of ligature-induced peri-implantitis around different types of endosseous implants with three different surfaces in the canine mandible.

Materials and Methods

Extractions and Implant Surgery. During the study, animals were under the supervision of a veterinary team (Laboratory Animal Resources Department, University of Texas Health Science Center) and were treated according to humane guidelines. The mandibular second, third, and fourth premolars of 14 healthy beagle dogs were extracted bilaterally. Three months later, three different submerged implants were placed on each side of the mandible (Fig 1). An HA, titanium plasma-sprayed (TPS), and titanium alloy (Ti-A) test implant were placed in a random anterior-posterior distribution. All implants were 10 mm in length and 4 mm in diameter. After an additional 3 months, abutments were connected. Three days later, metallic superstructures were placed to protect the implants from functional and parafunctional loading. Oral hygiene, consisting of tooth brushing (C.E.T., VRx Products, Harbour City, CA) and interproximal brushing and scaling with a graphite scaler (SteriOss, Yorba Linda, CA), was performed three times per week. No antimicrobial additives were used to prevent carry-over effect from the control to the experimental side. If necessary, animals were sedated every 2 weeks to ensure complete plaque and calculus removal.

Experimental Phase. After 4 weeks of healing, baseline readings, consisting of DNA from the deepest probing site at each implant (DMD_X, OmniGene, Cambridge, MA), were taken, and standardized radiographs (Ultra-speed, Eastman Kodak, Rochester, NY) were made. DNA samples were obtained with sterile paper points after careful supragingival plaque removal. Since no information could be found in the literature about the correlation of the level of microbes and the extent of infection, a number of statistical analyses, with different threshold levels, were performed. For example, the statistical analysis of Pg involved separating the DNA data into four categories ($< 6 \times 10^3$; 6.1×10^3 to 6×10^4; 6.01×10^4 to 6×10^5; $> 6 \times 10^5$); and a second analysis was based on Pg readings for control implants using only three categories ($< 6 \times 10^3$; 6.1×10^3 to 3.5×10^5; $> 3.5 \times 10^5$). For standardized radiographs, custom-made film holder/bite blocks (XCP, Rinn Corp, Elgin, IL) were manufactured. The experimental sides were chosen at random. Peri-implant inflammation was induced using braided cotton retraction cord (GingiBraid, VanR Dental Products, Oxnard, CA) without astringents on the experimental side of the mandible. Ligatures were placed subgingivally around the neck of the implants. Plaque control was maintained around control implants and discontinued on the experimental side of the mandible. If necessary, ligatures were replaced at the plaque control appointments. Standardized radiographs were repeated monthly.

Sacrifice. Three months after ligature placement, six dogs were sacrificed; the remaining eight dogs were euthanized at 6 months. In addition to standardized radiographs, a second DNA probe sample from the deepest site at each implant was taken at sacrifice (Fig 1) after supragingival plaque removal. After initial fixation in 10% formalin, the mandibles were block-resected, and the recovered segments with the implants were immersed in Poly/Lem Fixative (Polysciences, Warrington, PA).

Histology. Implants were separated by a buccolingual cut using an Isomet low-speed saw with a diamond blade (Buehler, Lake Bluff, IL). Subsequently, these segments were cut mesiodistally through the midline of each implant. Finally, two sections were obtained at a distance of 100 µm. A Leica 1600 microtome saw (Leica, Wetzlar, Germany), equipped with a diamond-coated blade, was used to procure these 15- to 20-µm-thick sections. Slides were prepared for light microscopy without prior demineralization. Dehydration was accomplished by graded methanols (70 to 100%). Samples were embedded by infiltration with Osteo-Bed media (Polysciences) and xylene and stained with toluidine blue O, basic fuchsin, and alizarin red.

The bone height and any subsequent vertical or horizontal bone loss were quantitated histometrically using the VISTA Bioquant System (R & M Biometrics, Nashville, TN). (It was possible to measure the amount of bone loss since the implants were placed with their top at the bone crest level.) Vertical bone loss (VBL) was computed. At the microscopic level, the presence of the HA coating was verified and the current thickness of hydroxyapatite coating (THA) at various levels of the implants was measured.

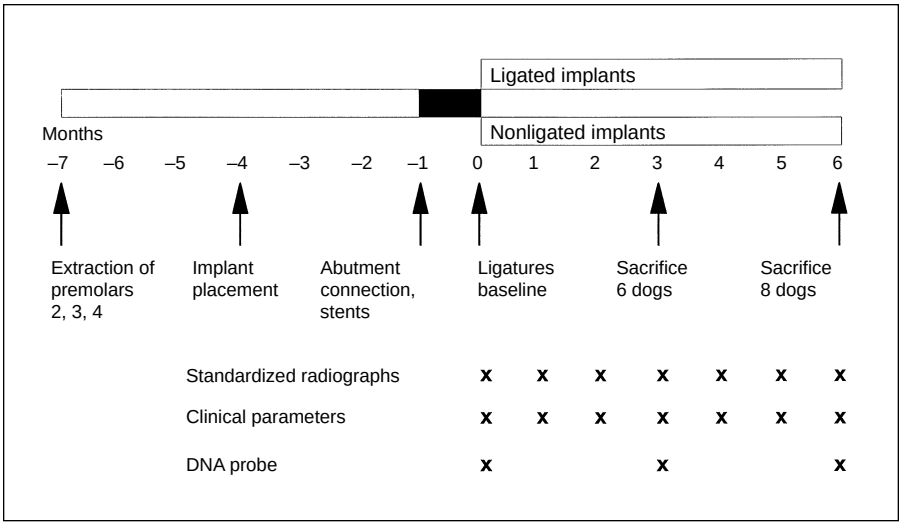

Fig 1 Study design.

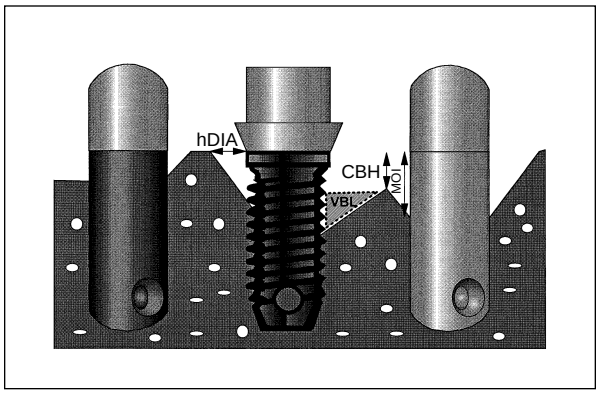

Fig 2 Schematic of histologic measurements at different implant types: horizontal distance from the implant to the most coronal point of the alveolar crest (hDIA); changes in crestal bone height (CBH); marginal changes in osseointegration (MOI); and area of vertical bone loss (VBL).

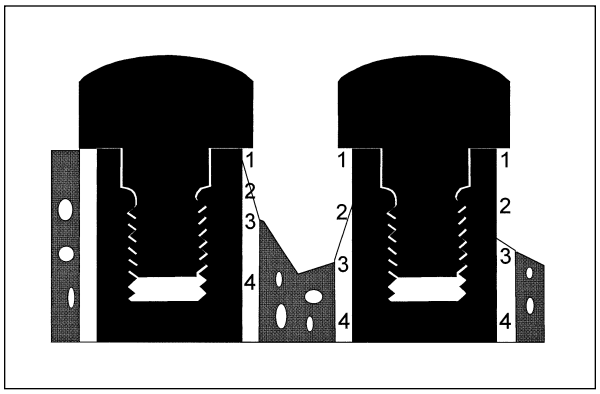

Fig 3 Schematic of HA coating assessment. Points of evaluation: point 1 = neck of implant; point 2 = one-half the distance between points 1 and 3; point 3 = most coronal bone-implant contact; point 4 = 3 mm apical to point 3.

The following measurements were taken (Fig 2):

- Vertical distance from the neck of the implant to the most coronal point of the crestal bone (CBH)
- Distance from the neck of the implant to the most coronal aspect of osseointegration (MOI)
- Horizontal distance from the implant to the most coronal point of the alveolar crest (hDIA)
- THA at four different locations (Fig 3)
- VBL, calculated using the measured distances

Radiography. After digitization and subtraction radiography, radiographs were analyzed by CADIA. To increase accuracy, only one examiner performed the radiographic analysis.[22] The area-of-interest (AOI), 16 × 16 pixels in size (0.60 mm^2), was defined on the baseline radiographs and placed adjacent to the implants, including the most coronal bone-to-implant contact. The AOI was placed approximately 0.1 mm away from the implant to avoid inherent errors produced by superimposition of the implant. Variation in pixel values of the subtraction images of an unchanged area were found to be between 4.5 and 8.5 gray values. Therefore, a threshold value between ± 9 and ± 17 was chosen to exclude 95% of the image noise and yield CADIA values representative of true changes in bone mineral content. Negative values represented a decrease and positive values an increase in radiographic density.

Statistics. When control and experimental values were compared at the same time points and a normal

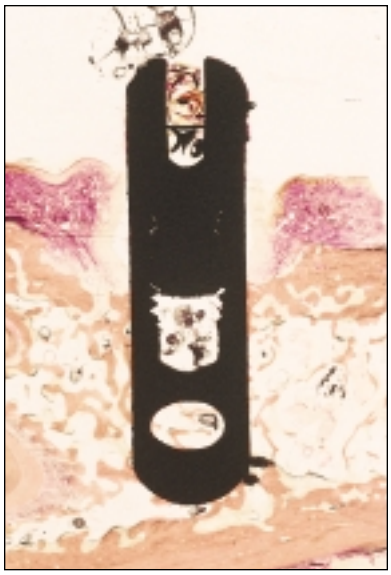

Fig 4a *(left)* Light micrograph of an unloaded, control HA implant at 6 months. Complication-free tissue integration of implant and abutment is noticeable (mesiodistal section, original magnification × 1.8; stained with toluidine blue O, basic fuchsin, and alizarin red).

Fig 4b *(right)* Light micrograph of an unloaded, experimental HA implant at 6 months. Typical signs of peri-implant breakdown around implant and abutment are apparent (mesiodistal section, original magnification × 1.8; stained with toluidine blue O, basic fuchsin, and alizarin red).

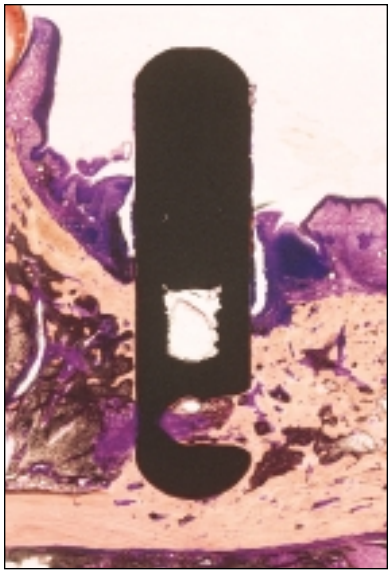

Fig 5a *(left)* Light micrograph of an unloaded, control TPS implant at 6 months. Complication-free tissue integration of implant and abutment is evident. Note loss of abutment because of histologic processing (artifact). (Mesiodistal section, original magnification × 1.8; stained with toluidine blue O, basic fuchsin, and alizarin red.)

Fig 5b *(right)* Light micrograph of an unloaded, experimental TPS implant at 6 months. Typical signs of peri-implant breakdown around implant and abutment are apparent (mesiodistal section, original magnification × 1.8; stained with toluidine blue O, basic fuchsin, and alizarin red).

distribution was present, the paired *t* test was used (histology, experimental versus control implants). When a normal distribution was not found, a Wilcoxon signed rank analysis (THA, CADIA, DNA) was performed. For comparisons over time, analysis of variance (ANOVA) and a post-hoc analysis, using a general linear model with least mean squares, was utilized. Differences among the implant types were analyzed by *F* approximation for Friedman test. When multiple comparisons were made, the *P* value was adjusted accordingly. Correlations were examined for parametric data (CAL,[30] histology) by Pearson correlation analysis, and for nonparametric data (CADIA) by Spearman correlation analysis.

Results

Three implants, one of each type, failed to integrate and were removed before the initiation of the experimental phase. All of the other 81 implants were deemed osseointegrated and clinically successful. Thirty-nine control implants revealed complication-free tissue integration (Figs 4a, 5a, and 6a). All 42 experimental implants showed typical signs of peri-implant lesions (Figs 4b, 5b, and 6b).

Microbiology. At the end of the study, the levels of all microbes tested were increased at all implants (Table 1). Microbial levels were analyzed by Wilcoxon's signed rank test with two different sets of

Table 1 DNA Probe Results for the Presence of Three Bacterial Species at Three Different Types of Implants at Baseline and at End of Study

	Porphyromonas gingivalis (× 1000)						*Provotella intermedia* (× 1000)						*Actinobacillus actinomycetemcomitans* (× 1000)					
	HA		TPS		Ti-A		HA		TPS		Ti-A		HA		TPS		Ti-A	
Time	Ctrl	Exp	Ctrl	Exp	Ctrl	Exp	Ctrl	Exp	Ctrl	Exp	Ctrl	Exp	Ctrl	Exp	Ctrl	Exp	Ctrl	Exp
3 Months																		
Dog 1																		
Baseline	ND	7.3	ND	ND	ND	ND	ND	8.2	7.5	ND	ND	ND	ND	ND	ND	ND	ND	ND
End of study	7.5	100	33	25	ND	> 600	ND	12	11	10	ND	43	ND	6.6	ND	6.9	ND	6.1
Dog 2																		
Baseline	14	ND	23	12	8.2	8	ND	ND	ND	ND	ND	ND	ND	ND	ND	ND	ND	ND
End of study	ND	61	ND	> 600	ND	210	ND	20	ND	140	ND	38	ND	ND	ND	6.3	ND	ND
Dog 3																		
Baseline	ND	ND	ND	ND	ND	13	ND	ND	ND	ND	ND	ND	ND	ND	ND	ND	ND	ND
End of study	ND	590	ND	> 600	13	12	ND	30	ND	10	ND	ND	ND	ND	ND	ND	ND	ND
Dog 4																		
Baseline	†	ND	ND	ND	ND	ND	†	ND	ND	ND	ND	ND	†	ND	ND	ND	ND	ND
End of study	†	23	130	8.2	470	28	†	ND	9.7	ND	13	ND	†	ND	ND	ND	ND	ND
Dog 5																		
Baseline	ND	90	ND	ND	ND	96	ND	ND	ND	ND	ND	18	ND	ND	ND	ND	ND	ND
End of study	ND	ND	ND	ND	ND	ND	ND	6.7	ND	ND	ND	6.6	ND	ND	ND	ND	ND	ND
Dog 6																		
Baseline	ND	ND	†	ND	ND	58	ND	ND	†	ND	ND	ND	ND	ND	ND	ND	ND	ND
End of study	400	55	†	480	> 600	> 600	37	8.1	†	29	51	40	ND	ND	ND	ND	ND	ND
6 Months																		
Dog 1																		
Baseline	ND	ND	ND	ND	20	ND	ND	ND	ND	ND	7.2	ND	ND	ND	ND	ND	ND	ND
End of study	ND	26	23	130	ND	> 600	ND	ND	ND	ND	ND	27	ND	ND	ND	ND	ND	ND
Dog 2																		
Baseline	ND	ND	ND	7.6	ND	ND	ND	ND	ND	ND	ND	ND	ND	ND	ND	ND	ND	ND
End of study	50	28	43	91	170	ND	13	ND	12	13	26	ND	ND	ND	ND	ND	ND	ND
Dog 3																		
Baseline	ND	ND	ND	ND	ND	ND	ND	ND	ND	ND	ND	ND	ND	ND	ND	ND	ND	ND
End of study	ND	74	ND	240	ND	440	ND	10	ND	10	ND	13	ND	ND	ND	ND	ND	ND
Dog 4																		
Baseline	54	ND	58	92	16	ND	12	ND	32	14	ND	ND	ND	ND	ND	ND	ND	ND
End of study	ND	52	170	31	46	110	ND	11	23	ND	11	10	ND	ND	ND	ND	ND	ND
Dog 5																		
Baseline	ND	120	ND	250	ND	6.5	ND	18	ND	55	ND	ND	ND	ND	ND	ND	ND	ND
End of study	98	> 600	ND	510	ND	76	18	37	ND	33	ND	40	ND	ND	ND	ND	ND	ND
Dog 6																		
Baseline	ND	ND	59	ND	†	ND	ND	10	ND	ND	†	ND	ND	ND	ND	ND	ND	ND
End of study	48	260	33	ND	†	48	18	12	24	ND	†	100	ND	ND	7.4	ND	ND	ND
Dog 7																		
Baseline	9.1	ND	ND	ND	12	52	ND	ND	10	ND	36	ND	ND	ND	ND	ND	ND	ND
End of study	84	530	ND	71	390	170	33	410	9.9	19	43	23	ND	21	ND	ND	ND	ND
Dog 8																		
Baseline	ND	ND	ND	ND	ND	ND	ND	ND	ND	ND	6.3	17	ND	ND	ND	ND	ND	ND
End of study	ND	150	ND	ND	ND	ND	ND	11	ND	ND	ND	ND	ND	ND	ND	ND	ND	ND

†No DNA test performed.
ND = not detectable (< 6000).
Ctrl = control; Exp = experimental.

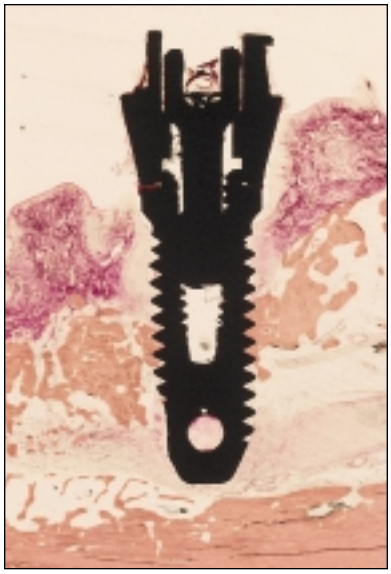

Fig 6a *(left)* Light micrograph of an unloaded, control Ti-A implant at 6 months. Complication-free tissue integration of implant and abutment is evident. Note most coronal bone-implant contact in area of first thread (mesiodistal section, original magnification × 1.8; stained with toluidine blue O, basic fuchsin, and alizarin red).

Fig 6b *(right)* Light micrograph of an unloaded, experimental Ti-A implant at 6 months. Typical signs of peri-implant breakdown around implant and abutment are noted (mesiodistal section, original magnification × 1.8; stained with toluidine blue O, basic fuchsin, and alizarin red).

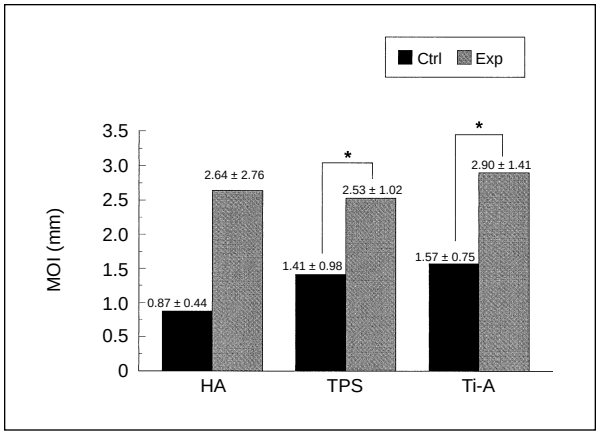

Fig 7 Marginal changes in osseointegration (MOI) at 3 months (n = 6; mean ± standard deviation). Significant increase for experimental TPS and Ti-A implants versus controls were noted (*P < .05).

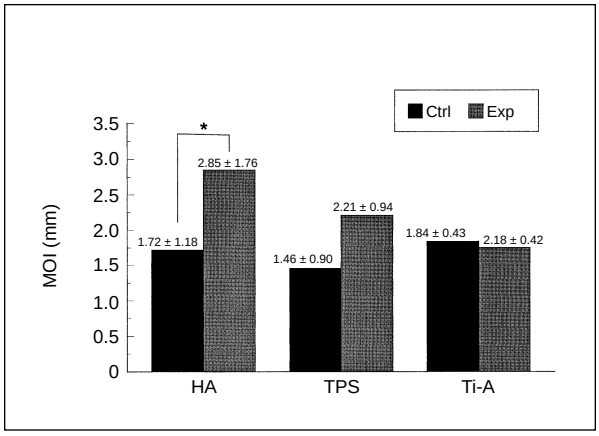

Fig 8 Marginal changes in osseointegration (MOI) at 6 months (n = 8; mean ± standard deviation). Experimental HA implants experienced significant loss compared to controls (*P < .05).

categories. The first analysis (four categories) detected significantly increased levels for Pg around experimental HA implants, when compared to baseline measurements at 6 months (P < .05). The second analysis (three categories) could not detect any significant difference in microbiota around the three different implant types. Aa was never present at the beginning of the study and showed a very low prevalence; it could only be detected 6 times out of 162 samples (less than 4%).

Histology. Histologic evaluations revealed a decrease in MOI for all implants at 3 and 6 months (Figs 7 and 8). Greater loss was noted at the experimental implants, and significant differences were noted between the control and experimental group for TPS and Ti-A at 3 months and for HA at 6 months (P < .05). However, F approximation for Friedman test revealed no significant differences among the three implant types. All implants lost CBH (Figs 9 and 10), and only Ti-A showed significant differences between control and experimental implants at 3 months (P < .05). No differences among the tested implants were noted for CBH. VBL was shown to be significantly greater for TPS at 6 months when control and experimental groups were compared (Figs 11 and 12). This was significantly different from the other two implant types (P < .025).

When the THA was evaluated (Fig 13), no difference between the 3- and 6-month data was detected. Therefore, the data were analyzed together. At point

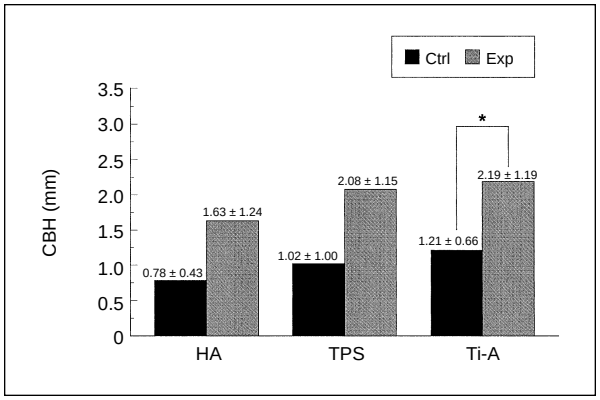

Fig 9 Changes in crestal bone height (CBH) at 3 months (n = 6; mean ± standard deviation). Experimental Ti-A implants exhibited a significant decrease in crestal bone level (*$P < .05$).

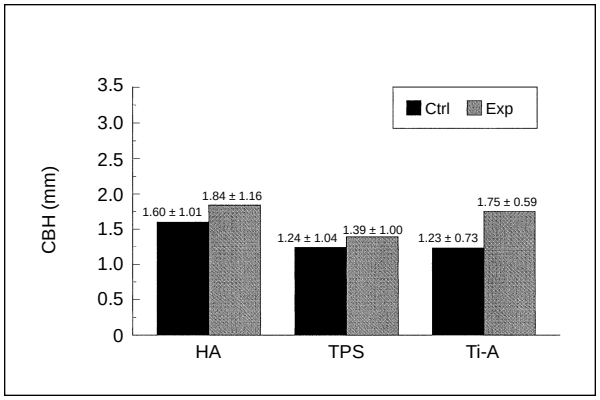

Fig 10 Changes in crestal bone height (CBH) at 6 months (n = 8; mean ± standard deviation). No significant changes between control and experimental groups were apparent.

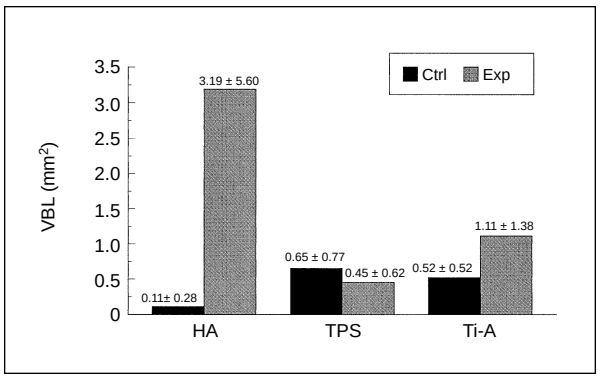

Fig 11 Area of vertical bone loss (VBL) at 3 months (n = 6; mean ± standard deviation). Despite noticeable increases at experimental HA implants, no statistically significant differences between control and experimental implants were detectable.

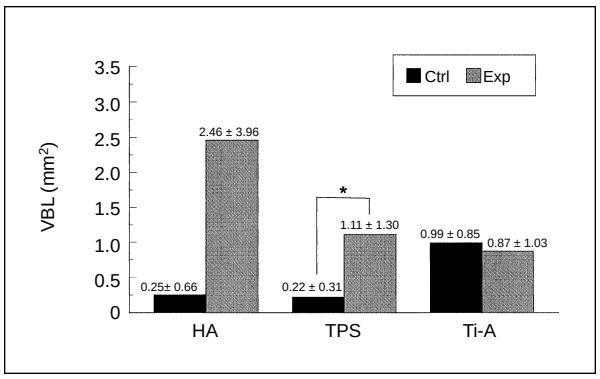

Fig 12 Area of vertical bone loss (VBL) at 6 months (n = 8; mean ± standard deviation). Although an increase was observed for experimental HA implants compared to controls, significant changes were only evident comparing experimental TPS implants versus controls (*$P < .05$).

2 (Fig 14), THA in the experimental group was decreased when compared to the control implants ($P < .05$). No differences at all other points of evaluation between control and experimental HA implants were apparent. It was noted, however, that in almost all cases, no HA coating could be detected at point 1. The thickness at points 3 and 4 ranged from 48.22 ± 9.18 µm to 54.14 ± 7.50 µm.

Radiology. CADIA values at 3 months (Fig 15) indicated a significant decrease in bone density for experimental compared to control implants ($P < .05$). The same trend was noted at 6 months (Fig 16), with only TPS showing statistically significant decreases in bone density between control and experimental implants. No difference among the tested implant types was detected at 3 and 6 months.

Correlations. High correlation of CAL to MOI for both control and experimental TPS and HA was found ($r = .71$ to $r = .94$, $P < .05$). At experimental Ti-A, high correlation for CAL to MOI was discovered ($r = .92$, $P < .05$). Moderate correlation was detected for mobility with MOI at experimental implants ($r = .58$ for TPS and HA, $P < .05$; $r = .76$ for Ti-A, $P < .05$). No correlations of PPD or CADIA to histologic parameters were found.

Discussion

In the present study, placement of cotton ligatures and cessation of oral hygiene to accelerate plaque formation resulted in the formation of a pocket that allowed for the establishment of pathologic subgingival microbiota. This reaction was associated with a deterioration of examined parameters in this study. The acute inflammatory tissue response to bacterial plaque accumulation seemed to represent a localized

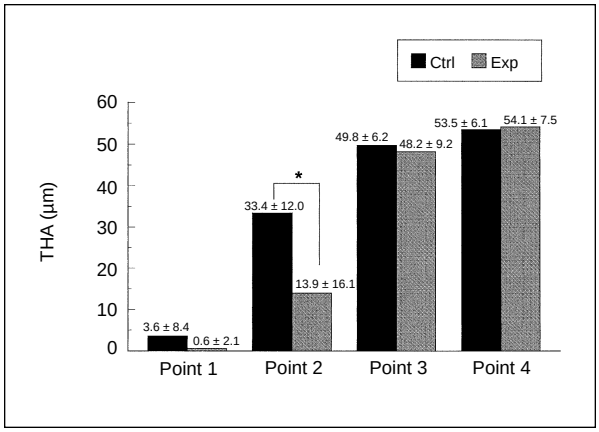

Fig 13 Thickness of HA coating (THA) at 3 and 6 months (mean ± standard deviation). Significant changes were detected between experimental and control implants at point 2 (*P < .05).

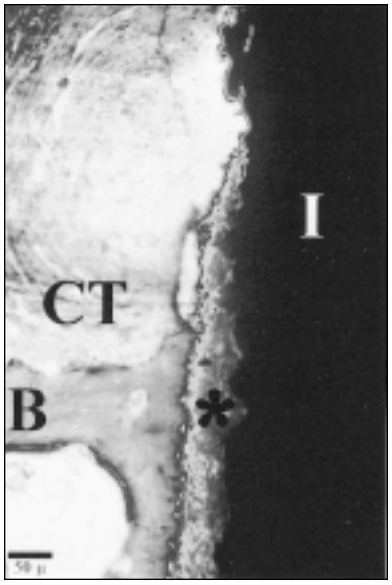

Fig 14 Hard and soft tissue interface of an unloaded, experimental HA implant at 6 months. I = implant; CT = connective tissue, B = bone; * = HA coating. Note resorption of HA coating above the most coronal bone-implant contact (mesiodistal section, original magnification × 50, bar = 50 µm; stained with toluidine blue O, basic fuchsin, and alizarin red).

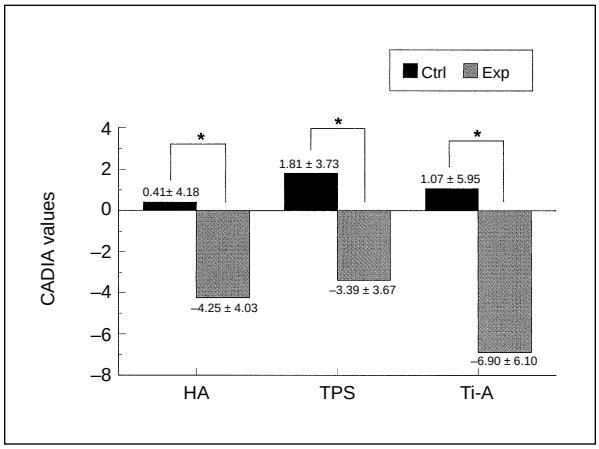

Fig 15 Computer-assisted densitometric image analysis (CADIA) at 3 months (n = 14; mean ± standard deviation). Statistical analysis revealed significant decreases of bone density at all experimental implants (*P < .05).

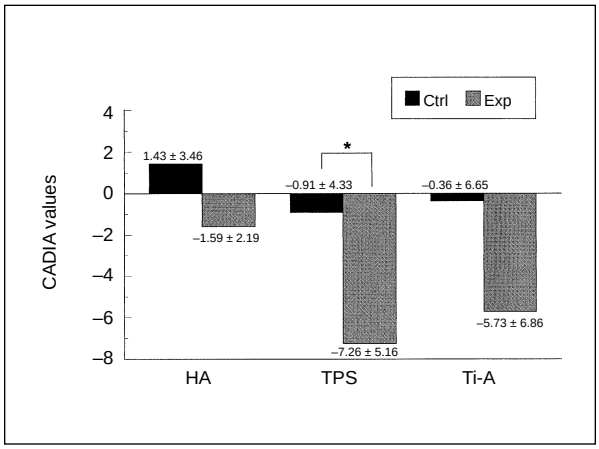

Fig 16 Computer-assisted densitometric image analysis (CADIA) at 6 months (n = 8; mean ± standard deviation). Although differences between control and experimental implants were noted, a statistically significant level was only reached at the TPS implant (*P < .05).

lesion, comparable to that encountered in advanced periodontal[25–27] as well as peri-implant[18,19,28,29] disease. Comparable observations have been reported in a study where cotton floss ligatures were placed at mandibular premolars in dogs with longstanding plaque and gingivitis.[31] It was concluded that the placement of the ligatures converted an established lesion to an advanced and progressively destructive lesion.[32]

When the three different implant types were compared by clinical parameters, no relevant differences among HA, TPS, or Ti-A could be found, either in the performance of the control implants or in the response to infection, as reported previously.[30] Compelling was the observation of this study that no consistent differences among the three different implant types in the extent of peri-implant breakdown were found at the histologic level. These findings sug-

gest a similar susceptibility and response of the evaluated implant types of induced peri-implantitis.

In this study, DNA analysis of three putative pathogens (Aa, Pg, Pi) revealed ambiguous findings since, of the two performed analyses, one showed no significance and the other showed significance. Because of the lack of information in the literature, one cannot favor one analysis over the other. Therefore, this study cannot answer the question of whether there is a significant impact of microbial colonization resulting from different surface characteristics based on the severity of peri-implant infection. However, generally increased levels have been previously reported at different types of endosseous implants.[6,9,12] Mombelli et al[6] studied the microbiota associated with failing implants in humans. They defined a failing implant as one displaying signs of deep pocketing, suppuration, and loss of alveolar bone. The unsuccessful sites harbored a microflora with a large proportion of gram-negative anaerobic rods (eg, black-pigmented bacteroides and fusobacterium species) as well as spirochetes. Control sites, ie, successful sites in the same patients, harbored sparse microbiota, which were dominated by coccoid cells. Similar findings were presented by Becker et al,[9] who observed that the pocket microbiota at failing implants in humans revealed moderate levels of Aa, Pg, and Pi.

Several studies have reported on ligature-induced peri-implant breakdown, comparing control and experimental implants in a split-mouth design.[20,28,29] Since the severity of peri-implant disease is the result of bacterial insult and individual host response, a direct comparison of different implant types in the same animal would seem to be crucial in evaluating characteristic tissue responses. Therefore, conclusions drawn in several anecdotal reports, associating HA implants with higher susceptibility to peri-implantitis, may be questionable.[33,34] In this study, no difference among the three tested implant types in terms of the extent of peri-implant breakdown was found at the histologic level. This indicates similar susceptibility of the evaluated implants to induced peri-implantitis.

When THA was assessed at points 3 and 4, no apparent loss over time of HA coating was noted. The measured values confirm the dimensions given by the manufacturer of approximately 50-µm thickness. The significant increase of HA resorption at point 2 conforms to previously reported observations.[21,22,35] Oral hygiene procedures and/or subclinical inflammation may have contributed to the decrease of THA at points 1 and 2.

Several studies suggested detection of early loss of integration at dental implants by digital subtraction radiography[36] and CADIA.[23,24] At 6 months, only experimental TPS implants showed a significant decrease in bone density when compared to controls. The lack of statistically significant changes for HA and Ti-A implants is most likely the result of a reduced number of subjects evaluated. No difference among the implant types was noted. However, large standard deviations were detected in this CADIA analysis. Therefore, minor CADIA changes should only be interpreted in conjunction with other measurements. CAL has been shown to have the highest correlation of all evaluated clinical parameters to the histologic data. Therefore, the clinical evaluation of peri-implant disease should focus primarily on CAL measurements.

Conclusion

Side-by-side comparison of the three different implant types revealed similar susceptibility to induced peri-implantitis. In comparing clinical, microbial, and histologic evaluation of peri-implant anatomy and pathology, CAL has been shown to be the best clinical parameter, exhibiting the highest correlation between clinical and histologic status. Meticulous oral hygiene, even around endosseous implants, appears to be a major prerequisite for successful implant treatment.

Acknowledgments

We would like to acknowledge William R. Wagner, PhD, for his continuous support and expertise. We gratefully acknowledge Sonja A. Bustamante, HT (ASCP), for her valuable contributions throughout this study. We would also like to thank Richard J. Haines, DVM, and Robyn K. Miller, RVT, LATG, for their help during the experimental part of the project, Pirkka V. Nummikoski, DDS, for his assistance with CADIA evaluation, John D. Schoolfield, MS, for statistical analyses, and Brian L. Mealey, DDS, MS, for his expertise. This investigation was supported by grants from Calcitek Inc, Carlsbad, California, and the Department of Periodontics at the University of Texas Health Science Center, San Antonio, Texas.

References

1. Listgarten MA, Helldén L. Relative distribution of bacteria at clinically healthy and periodontally diseased sites in humans. J Clin Periodontol 1978;5:115–132.
2. Savitt ED, Socransky SS. Distribution of certain subgingival microbial species in selected periodontal conditions. J Periodontal Res 1984;19:111–123.
3. Slots J, Bragd L, Wikstrom M, Dahlén G. The occurrence of *Actinobacillus actinomycetemcomitans, Bacteroides gingivalis* and *Bacteroides intermedius* in destructive periodontal disease in adults. J Clin Periodontol 1986;13:570–577.
4. Slots J, Listgarten MA. *Bacteroides gingivalis*, *Bacteroides intermedius* and *Actinobacillus actinomycetemcomitans* in human periodontal diseases. J Clin Periodontol 1988;15:85–93.

5. Dzink JL, Socransky SS, Haffajee AD. The predominant cultivable microbiota of active and inactive lesions of destructive periodontal diseases. J Clin Periodontol 1988;15:316–323.
6. Mombelli A, Van Oosten MAC, Schürch E, Lang NP. The microbiota associated with successful or failing osseointegrated titanium implants. Oral Microbiol Immunol 1987;2:145–151.
7. Nakou M, Mikx FHM, Oosterwaal PJM, Kruijsen JCWM. Early microbial colonization of permucosal implants in edentulous patients. J Dent Res 1987;66:1654–1657.
8. Mombelli A, Buser D, Lang NP. Colonization of osseointegrated titanium implants in edentulous patients. Early results. Oral Microbiol Immunol 1988;3:113–120.
9. Becker W, Becker BE, Newman MG, Nyman S. Clinical and microbiologic findings that may contribute to dental implant failure. Int J Oral Maxillofac Implants 1990;5:31–38.
10. Ong ES, Newman HN, Wilson M, Bulman JS. The occurrence of periodontitis-related microorganisms in relation to titanium implants. J Periodontol 1992;63:200–205.
11. Leonhardt A, Adolfsson B, Lekholm U, Wikstrom M, Dahlén G. A longitudinal microbiological study on osseointegrated titanium implants in partially edentulous patients. Clin Oral Implants Res 1993;4:113–120.
12. Mombelli A, Marxer M, Garberthüel T, Grunder U, Lang NP. The microbiota of osseointegrated implants with a history of periodontal disease. J Clin Periodontol 1995;22:124–130.
13. van Winkelhoff AJ, de Graaff J. Microbiology in the management of destructive periodontal disease. J Clin Periodontol 1991;18:406–410.
14. Gould TRL, Brunette DM, Westbury L. The attachment mechanisms of epithelial cells to titanium in vitro. J Periodontal Res 1981;16:611–616.
15. Linder L, Albrektsson T, Brånemark P-I, Hansson H-A, Ivarsson B, Jönsson U, Lundström I. Electron microscopic analysis of the bone-titanium interface. Acta Orthop Scand 1983;54:45–52.
16. Listgarten MA, Lang NP, Schroeder HE, Schroeder A. Periodontal tissues and their counterparts around endosseous implants. Clin Oral Implants Res 1991;2:1–19.
17. Berglundh T, Lindhe J, Ericsson I, Marinello CP, Liljenberg B, Thomsen P. The soft tissue barrier at implants and teeth. Clin Oral Implants Res 1991;2:81–90.
18. Buser D, Weber HP, Donath K, Fiorellini JP, Paquette DW, Williams RC. Soft tissue reactions to non-submerged unloaded titanium implants in beagle dogs. J Periodontol 1992;63:226–236.
19. Ericsson I, Lindhe J. Probing depth at implants and teeth. An experimental study in the dog. J Clin Periodontol 1993;20:623–627.
20. Lang NP, Wetzel AC, Stich H, Caffesse RC. Histologic probe penetration in healthy and inflamed peri-implant tissues. Clin Oral Implants Res 1994;5:191–203.
21. Richter EJ, Jansen V, Spiekermann H, Jovanovic SA. Langzeitergebnisse von IMZ-und TPS-Implantaten im interoforaminalen Bereich des zahnlosen Unterkiefers. Dtsch Zahnärztl Z 1992;47:449–454.
22. Jovanovic SA, Kenney EB, Carranza FA, Donath K. The regenerative potential of plaque-induced peri-implant bone defects treated by a submerged membrane technique: An experimental study. Int J Oral Maxillofac Implants 1993;8:13–18.
23. Brägger U, Pasquali L, Rylander H, Carnes D, Kornman KS. Computer-assisted densitometric image analysis in periodontal radiography. A methodological study. J Clin Periodontol 1988;15:27–37.
24. Brägger U. Radiographic parameters for the evaluation of peri-implant tissues. Periodontology 2000 1994;4:87–97.
25. Svanberg G, Lindhe J. Vascular reactions in the periodontal ligament incident to trauma from occlusion. J Clin Periodontol 1974;58:58–69.
26. Ericsson I, Lindhe J, Rylander H, Okamoto H. Experimental periodontal breakdown in the dog. Scand J Dent Res 1975;83:189–192.
27. Ericsson I, Lindhe J. Lack of significance of increased tooth mobility in experimental periodontitis. J Periodontol 1984;55:447–452.
28. Berglundh T, Lindhe J, Marinello C, Ericsson I, Liljenberg B. Soft tissue reaction to de novo plaque formation on implants and teeth. Clin Oral Implants Res 1992;3:1–8.
29. Lindhe J, Berglundh T, Ericsson I, Liljenberg B, Marinello C. Experimental breakdown of peri-implant and periodontal tissues. A study in the beagle dog. Clin Oral Implants Res 1992;3:9–16.
30. Tillmanns HWS, Hermann JS, Cagna DR, Meffert RM. Evaluation of three different dental implants in ligature-induced peri-implantitis in the beagle dog. Part I. Clinical evaluation. Int J Oral Maxillofac Implants 1997;12:611–620.
31. Schroeder HE, Lindhe J. Conversion of stable established gingivitis in the dog into destructive periodontitis. Arch Oral Biol 1975;20:775–782.
32. Page RC, Schroeder HE, Pathogenesis of inflammatory periodontal disease. A summary of current work. Lab Invest 1976;34:235–249.
33. Johnson BW. HA-coated dental implants: Long-term consequences. J Calif Dent Assoc 1992;20(6):33–41.
34. Kirsch A. Solutions for specific soft tissue situations. Int J Oral Maxillofac Implants 1994;9(suppl):30–38.
35. Krauser J, Berthold P, Tamary I, Seckinger R. A scanning electron microscopy study of failed endosseous root formed dental implants [abstract #65]. J Dent Res 1991;70:274.
36. Jeffcoat MK, Reddy MS, van den Berg HR, Bertens E. Quantitative digital subtraction radiography for the assessment of peri-implant bone change. Clin Oral Implants Res 1992;3:22–27.